Electronic Supplementary Information (ESI)

Cd(II) Based Metal-Organic Framework Behaving as Schottky Barrier Diode

Biswajit Bhattacharya,[a] Animesh Layek,[b] Md. Mehboob Alam,[c] Dilip Kumar Maity,[a] Swapan Chakrabarti,[c,*] Partha Pratim Ray,[b,*] and Debajyoti Ghoshal[a,*]

[a]Department of Chemistry, Jadavpur University, Jadavpur, Kolkata, 700 032, India.

[b]Department of Physics, Jadavpur University, Jadavpur, Kolkata, 700 032, India.

[c]Department of Chemistry, University of Calcutta, Kolkata, 700 009, India.

Table of Contents

Experimental Section:

Materials

trans 4,4′-azobispyridine (azbpy) was synthesized by the procedure reported earlier.[1] High purity cadmium(II) nitrate tetrahydrate and 5-hydroxyisophthalic acid were purchased from Sigma-Aldrich Chemical Co. Inc. and used as received. All other chemicals including solvents were of AR grade and used as received.

Synthesis of $\{[Cd_2(azbpy)_2(HO\text{-}1,3\text{-}bdc)_2].(azbpy)(H_2O)\}_n$, Cd-MOF (1)

An aqueous solution (3 ml) of disodium salt of 5-hydroxyisophthalic (HO-1,3-bdc) (0.045 g, 0.2 mmol) was mixed to a ethanolic solution of 4,4′-azobipyridine (azbpy) (0.037 g, 0.2 mmol) and stirred for 20 min to mix it well. $Cd(NO_3)_2.4H_2O$ (0.62 mg, 0.2 mmol) was dissolved in H_2O (3 mL), and this Cd(II) solution was slowly and carefully layered with the above mixed-ligand solution by using buffer solution (1 mL; 1:1 of H_2O and EtOH). Orange block-shaped crystals were obtained after 10 days. The reddish block crystals suitable for X-ray studies were obtained in approximately 78% yield after 15 days. The bulk samples of Cd-MOF (**1**) have been synthesized in powder form by the direct mixing of ligand mixture with the aqueous solution of metal salt solution followed by overnight stirring. This bulk powder sample was used for all physical measurements, conductivity as well as device fabrication. Elemental analysis, calculated for $C_{46}H_{34}Cd_2N_{12}O_{11}$ (M_r = 1155.67): C 47.81; H 2.97; N 14.54. Found in single crystal of Cd-MOF (**1**): C 47.87, H 2.88, N 14.51; and in powder form of Cd-MOF (**1**) C 47.95, H 2.83, N 14.62.

Physical Measurements

Microanalyses (C, H, N) were performed using a Perkin–Elmer 240C elemental analyzer. Infrared spectra (4000–400 cm^{-1}) were taken on KBr pellet, using Perkin–Elmer Spectrum BX-II IR spectrometer. Thermal analysis (TGA) was carried out on a METTLER TOLEDO TGA 850 thermal analyzer under nitrogen atmosphere (flow rate: 50 cm^3 min^{-1}) at the temperature range 30-500º C with a heating rate of 2º C/min. Solid state electronic absorption spectra were recorded on a Hitachi UV–Vis (Model U-3501) spectrophotometer.

Single Crystal X-ray Diffraction

X-ray single crystal data collection of Cd-MOF (**1**) were performed at room temperature using Bruker APEX II diffractometer, equipped with a normal focus, sealed tube X-ray source with graphite monochromated Mo-Kα radiation (λ= 0.71073Å). The data were integrated using SAINT program and the absorption corrections were made with SADABS. The structure was solved by SHELXS 97[2] using Patterson method and followed by successive Fourier and difference Fourier synthesis. Full matrix least-squares refinements were performed on F^2 using SHELXL-97[2] with anisotropic displacement parameters for all non-hydrogen atoms. All the hydrogen atoms were fixed geometrically by HFIX command and placed in ideal positions in case of Cd-MOF (**1**). Calculations were carried out using SHELXS 97,[2] SHELXL 97[2] and PLATON v1.15.[3]

Method of conductivity measurement

To measure the conductivity of Cd-MOF (**1**) in solid state, a thin film technique was adopted. The Cd-MOF (**1**) was mixed with DMF and was sonicated for half an hour's to get the well dispersed phase. Then using this dispersed phase, thin film deposition was done by spin coating technique using SCU-2007 spin coating unit. The thin film was spun at 1600 rpm for 2 minutes on to the pre-cleaned (with acetone, ethanol and distilled water accordingly by ultra-sonicator) glass substrate. To evaporate the solvent, as-deposited thin film was annealed under vacuum at 170 °C for 10 minutes. The thickness of the film was measured by surface profiler (make: ZETA Instrument). Thereafter, the Aluminium electrodes were deposited on to the film through shadow mask by Vacuum Coating Unit 12A4D of Hindhivac under low pressure of 10^{-6} m-barr. The dimensions of the Aluminium electrodes are of 9 mm × 1 mm with a gapping of 1 mm between two electrodes (Scheme S1). The mask was adjusted well, to maintain the dimension of the effective film with 9 mm × 1 mm effective area. Afterward, the electrodes were connected with a Keithley 2400 source meter by two-probe contact to measure the resistance vis-à-vis, conductivity measurement by monitoring the current-voltage (I-V) characteristic profile with different applied voltages. All these procedure had been performed under room temperature and in open atmosphere. Investigating the slope of I-V characteristic curve (Fig. S2) and considering the dimension of the film (effective length = l, area of cross section = $a \times d$) conductivity was measured with the help of equation:

$$\sigma = \left(\frac{\Delta I}{\Delta V}\right)\left(\frac{l}{ad}\right)$$

Where, σ is the conductivity, *l* is 1 mm, *a* is 9 mm. The thickness of the film (*d*) was measured as ~ 400 nm by the surface profiler.

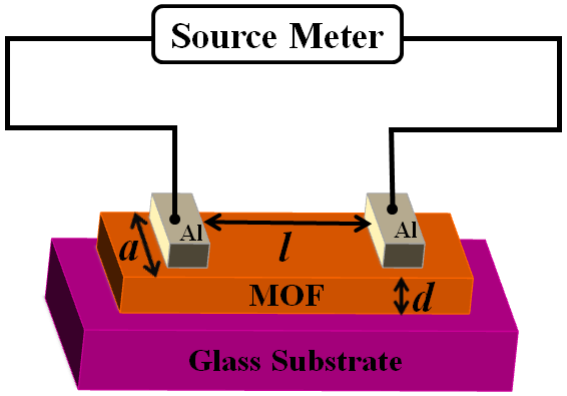

Scheme S1. Schematic representation of Glass substrate/ Cd-MOF (**1**)/Metal based thin film.

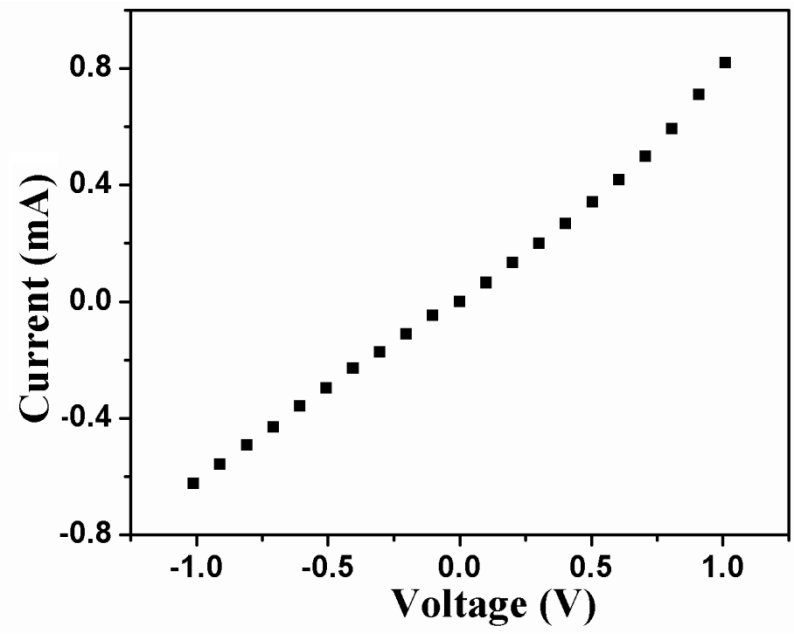

Fig. S1 Current-voltage plot for conductivity measurement of Cd-MOF (**1**).

Device Fabrication

Prior to Schottky device fabrication, indium tin oxide (ITO) coated glass substrate was washed successively with ethanol, acetone and de-ionized water repeatedly in sequence and dried within a vacuum chamber. For the deposition of thin active layer, dispersed solution of Cd-MOF (**1**) composites was prepared with DMF by ultrasonication technique. As the desire dispersed solution was obtained, thin film was deposited by spin coating on to the ITO substrate with the help of SCU-2007 spin coating unit, by spinning at 1600 rpm for 2 minutes. To evaporate the solvent, as-deposited thin film was annealed under vacuum at 170 °C for 10 minutes. Contact electrode was deposited from 99.99% pure Aluminium onto the composite films by vacuum thermal evaporation technique. The geometrical configuration of ITO/ Cd-MOF (**1**)/Al Schottky diode is the sandwich, as given in scheme S2. The effective diode contact area is maintained at 7.065 x 10^{-3} cm^2 by the shadow mask. After the deposition of metal electrode, current voltage characteristic of the Schottky Diode was measured by a Keithley 2400 sourcemeter, interfaced with PC.

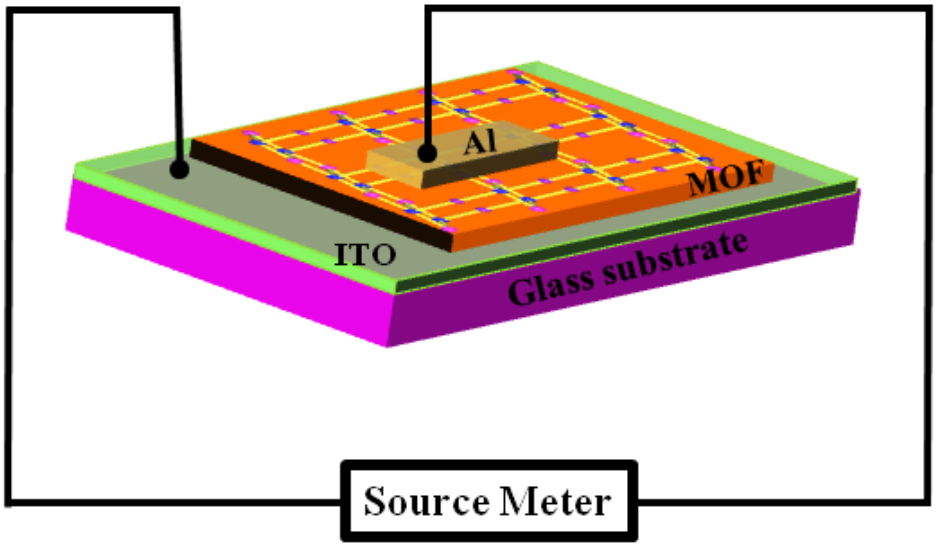

Scheme S2. Schematic representation of ITO/ Cd-MOF (**1**)/Metal based Schottky barrier diode under biased condition.

Theoretical Methods

Band structure calculations: The band structure calculations along with the theoretical justification of the optical absorption spectrum have been performed with meta-GGA functional, TB09,[4] in combination with double zeta polarized (DZP) basis functions on all the atoms present in the unit cell of the Cd-MOF (**1**). The K-point sampling in a 3D Monkhorst-Pack grid was done with 10 x 10 x10 points and the chosen mesh cut-off energy was 150 Rydberg. The software used is ATK 12.8.2.[5] In the band structure calculation of the Cd-MOF (**1**), the suggested route to the Brillouin zone, that is, the connecting symmetric k-points compatible with the triclinic Bravais lattice, was found to be Γ, Z, X and Y. The energy band structure as depicted in the Fig. 2 is scaled with respect to the Fermi level of the system.

Graphical details of Fig. 2: At first, the band structure was computed for the 10 bands lying above the Fermi level (E_F), from which only the four bands above the E_F and the two bands below the E_F were extracted separately. These two plots were then appended to get this final plot. The valence bands are found to be more closely spaced than the conduction bands. For this reason, we have plotted the conduction and valence bands at an energy gap of 0.002 eV and 0.0002 eV, respectively. In this plot, the E_F is set to zero.

Optical absorption spectra: The evaluation of the theoretical optical absorption spectra has been done following Kubo-Greenwood approximation.[6] Within this approximation the susceptibility tensor can be expressed as

$$\chi_{ij}(\omega) = -\frac{e^2\mathrm{h}^4}{m^2\varepsilon_0 V\omega^2}\sum_{nm}\frac{f(E_m)-f(E_n)}{E_{nm}-\mathrm{h}\omega-i\mathrm{h}\Gamma}\pi^i_{nm}\pi^j_{mn}$$

Where, π^i_{nm} π^j_{nm} are the components of the dipole matrix element between the state *n* and *m* while *V*, *Γ* and *f* represent the volume, broadening and the Fermi function, respectively.

According to the linear response theory, the dielectric constant in terms of susceptibility tensor can be expressed as

$$\varepsilon_r(\omega) = 1 + \chi(\omega)$$

In the next step, the frequency dependent dielectric constant is split into the real and the imaginary part,

$$n + i\kappa = \sqrt{\varepsilon_r}$$

where the real part is associated with the refractive index (n) of the medium and the imaginary part gives the extinction coefficient (κ) with

$$\kappa = \sqrt{\frac{\sqrt{\varepsilon_1^2 + \varepsilon_2^2} - \varepsilon_1}{2}}$$

Finally, the optical absorption coefficient can be evaluated by the formula, $\alpha_a = 2\frac{\omega}{c}\kappa$, here c is the velocity of the light.

Tables related to X-ray structure:

Table S1. Crytallographic and Structural Refinement Parameters of Cd-MOF (**1**).

Formula	$C_{46}H_{34}Cd_2N_{12}O_{11}$
Formula Weight	1155.67
Crystal System	Triclinic
Space group	$P\bar{1}$
a/ Å	10.2812(4)
b/Å	13.6284(5)
c/ Å	16.8750(7)
α/°	85.265(2)
β/°	75.138(2)
γ/°	81.491(2)
V/ Å^3	2257.75(15)
Z	2
D_c/ g cm^{-3}	1.700
μ /mm^{-1}	1.019
F(000)	1156
θ range/°	1.3-27.5
Reflections collected	37096
Unique reflections	10293
Reflections $I > 2\sigma(I)$	5765
R_{int}	0.075
goodness-of-fit (F^2)	0.99
$R1$ ($I > 2\sigma(I)$) [a]	0.0534
$wR2(I > 2\sigma(I))$ [a]	0.1100
Δρ max/min/e Å^3	-0.71, 0.83

[a] $R_1 = \Sigma \big| |F_o| - |F_c| \big| / \Sigma |F_o|$, $wR_2 = [\Sigma (w (F_o^2 - F_c^2)^2) / \Sigma w (F_o^2)^2]^{1/2}$

Table S2. Selected Bond Lengths (Å) and Bond Angles (°) for Cd-MOF (**1**).

Cd1-O1	2.294(3)	Cd1-O6	2.411(3)
Cd1-O7	2.367(3)	Cd1-N5	2.319(4)

Cd1-N8	2.318(4)	Cd1-O8^{a}	2.285(3)
Cd1-O9^{a}	2.759(3)	Cd2-O2	2.266(3)
Cd2-N1	2.311(4)	Cd2-O3^{a}	2.396(3)
Cd2-O4^{a}	2.371(3)	Cd2-O9^{a}	2.302(3)
Cd2-N4^{b}	2.341(4)		
O1-Cd1-O6	87.74(11)	O2-Cd2-N1	93.31(14)
O1-Cd1-O7	140.65(12)	O2-Cd2-O3^{a}	141.83(11)
O1-Cd1-N5	85.91(13)	O2-Cd2-O4^{a}	87.68(12)
O1-Cd1-N8	88.48(16)	O2-Cd2-O9^{a}	126.40(12)
O2-Cd2-N4^{b}	89.64(15)	O1-Cd1-O8^{a}	132.32(12)
O1-Cd1-O9^{a}	81.96(10)	O3^{a}-Cd2-N1	89.95(14)
O6-Cd1-O7	53.94(11)	O4^{a}-Cd2-N1	99.43(13)
O6-Cd1-N5	86.10(14)	O9^{a}-Cd2-N1	87.80(13)
O6-Cd1-N8	96.66(14)	N1-Cd2-N4^{b}	174.11(15)
O6-Cd1-O8^{a}	139.42(11)	O3^{a}-Cd2-O4^{a}	54.33(11)
O6-Cd1-O9^{a}	169.51(10)	O3^{a}-Cd2-O9^{a}	91.70(11)
O7-Cd1-N5	98.55(13)	O7-Cd1-N8	87.67(15)
O3^{a}-Cd2-N4^{b}	90.90(14)	O4^{a}-Cd2-O9^{a}	144.91(11)
O7-Cd1-O8^{a}	86.93(11)	O7-Cd1-O9^{a}	136.55(10)
O4^{a}-Cd2-N4^{b}	85.78(15)	N5-Cd1-N8	173.65(15)
O9^{a}-Cd2-N4^{b}	86.34(16)	O8^{a}-Cd1-N5	90.17(14)
O9^{a}-Cd1-N5	91.13(13)	O8^{a}-Cd1-N8	91.42(15)
O9^{a}-Cd1-N8	85.13(14)	O8^{a}-Cd1-O9^{a}	50.59(10)

Symmetry Code: *a* = -1+x, y, z; *b* = x, -1+y, z.

Table S3. Hydrogen bonding interactions (Å, °) of Cd-MOF (**1**).

D-H…A	D-H	H…A	D…A	<D-H...A
O1W-1WA…O6^{i}	0.8500	1.8900	2.680(5)	154.00
O1W-1WB…O3^{i}	0.8500	1.8700	2.677(5)	158.00
O10-H10...O1W^{ii}	0.8200	2.1200	2.672(5)	125.00

Symmetry code: i = 2-x, 1-y, -z; ii = x, y, 1+z.

Table S4. π-π interactions in Cd-MOF (**1**).

ring(i) → ring(j)	distance of centroid(i)	dihedral angle	distance between the

	from ring(j),(Å)	(i,j) (deg)	(i,j) ring centroids,(Å)
R(1)→ R(3)^{i}	3.860(3)	9.3(3)	3.682(2)
R(2)→ R(4)^{ii}	3.535(3)	2.1(3)	3.428(2)
R(2)→ R(8)^{iii}	4.254(4)	9.5(3)	3.644(3)
R(3)→ R(1)^{i}	3.860(3)	9.3(3)	3.452(2)
R(4)→ R(2)^{iv}	3.536(3)	2.1(3)	3.401(2)
R(4)→ R(7)^{i}	3.816(4)	9.7(4)	3.640(3)
R(5)→ R(5)^{v}	3.962(3)	0	3.695(2)
R(6)→ R(6)^{vi}	3.759(3)	0	3.680(2)
R(7)→ R(4)^{i}	3.816(4)	9.7(4)	3.413(2)
R(7)→ R(7)^{vii}	3.911(5)	0	3.597(3)
R(8)→ R(2)^{viii}	4.255(4)	9.5(3)	3.383(2)
R(8)→ R(8)^{ix}	3.801(5)	0	3.584(3)

Symmetry code: (i) = x, y, z; (ii) = x, 1+y, z; (iii) = -1+ x, 1+y, z; (iv) x, -1+y, z; (v) 2-x, 1-y, -z; (vi) = 2-x, 1-y, 1-z; (vii) = 2-x, -y, 1-z; (viii) = 1+ x, -1+y, z; (ix) 2-x, -y, -z.

R(i)/R(j) denotes the ith/jth rings: R(1) = N(1)/C(17)/C(18)/C(19)/C(20)/C(21); R(2) = N(4)/C(24)/C(23)/C(22)/C(26)/C(25); R(3) = N(5)/C(27)/C(28)/C(29)/C(30)/C(31); R(4) = N(8)/C(32)/C(33)/C(34)/C(35)/C(36); R(5) = C(2)/C(3)/C(4)/C(5)/C(6)/C(7); R(6) = C(10)/C(11)/C(12)/C(13)/C(14)/C(15); R(7) = N(9)/C(37)/C(38)/C(39)/C(40)/C(41); R(8) = N(12)/C(44)/C(43)/C(42)/C(46)/C(45).

Figures related to single crystal X-ray structure and the characterization of Cd-MOF (**1**)**:**

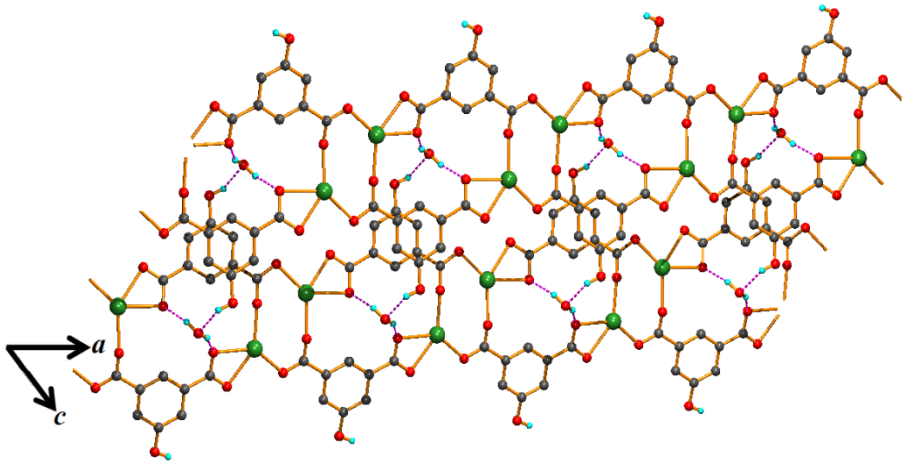

Fig. S2 Metal-carboxylate ladder chains stitched by lattice water molecules in Cd-MOF (**1**) (azbpy has been omitted for clarity).

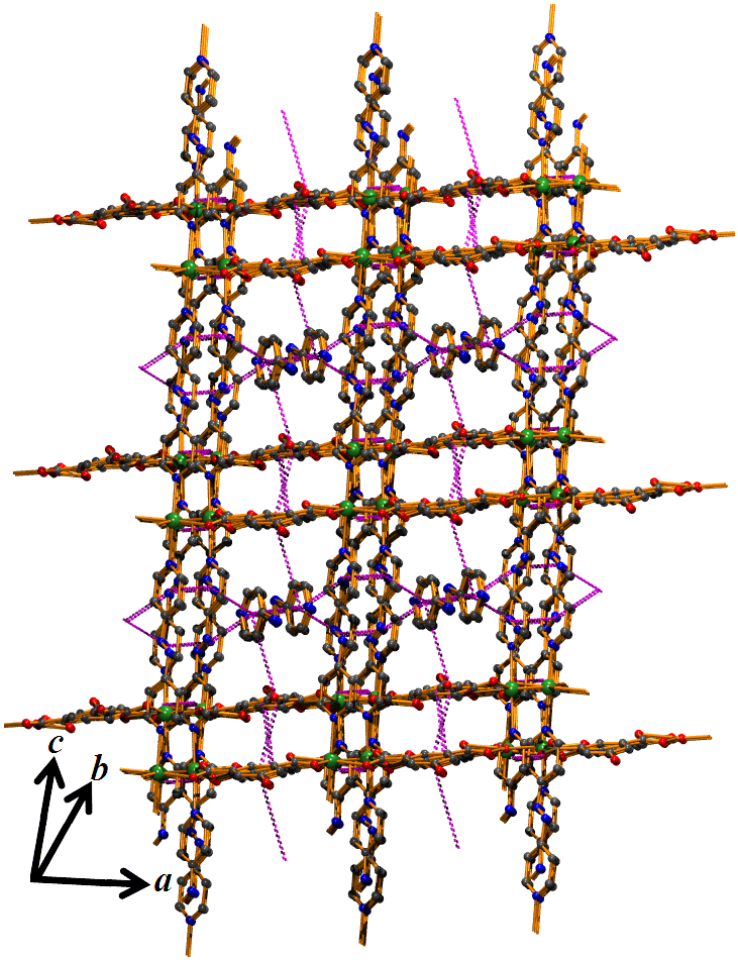

Fig. S3 Supramolecular 3D arrangement in Cd-MOF (**1**) (π-π interactions: pink dotted lines).

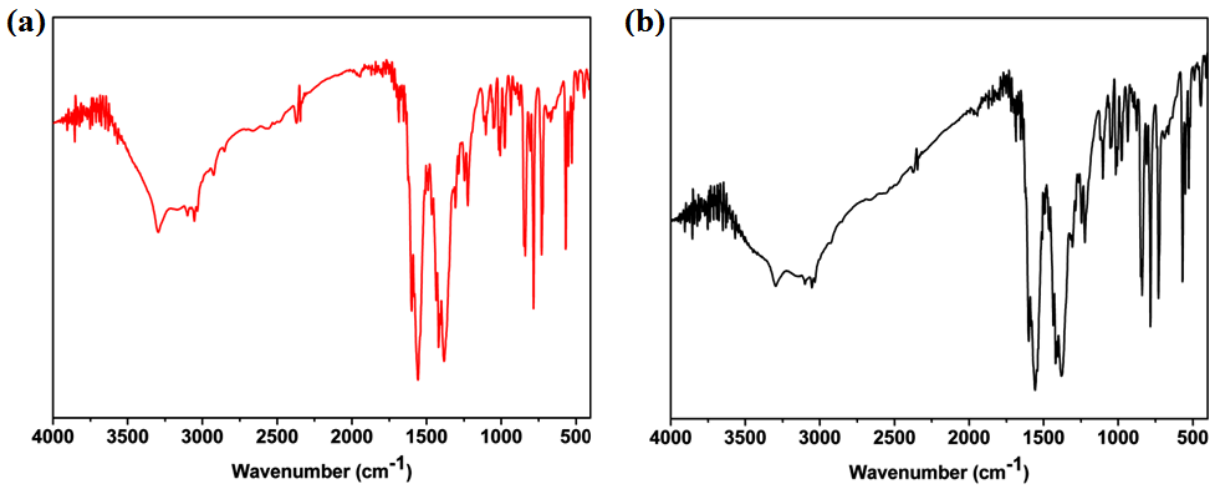

Fig. S4 IR spectra of Cd-MOF (**1**) (cm^{-1}) in (a) single crystal form and (b) bulk powder form. ν(N=N), 1599; ν(O-H), 3200-3600; ν(C-O), 1310-1220; ν(CH-Ar), 3100-2900 and ν(C=C), 1600-1380.

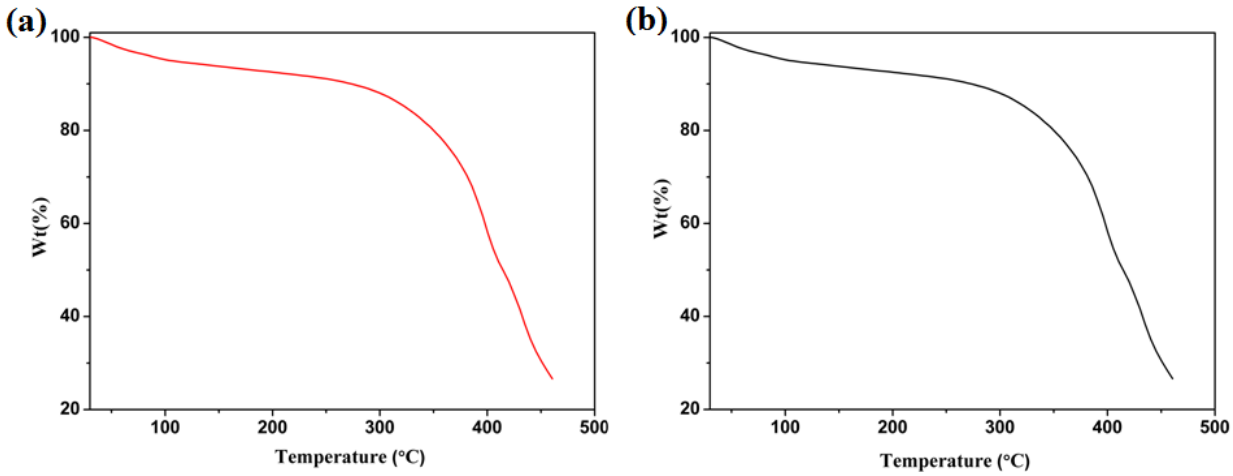

Fig. S5 TGA of the Cd-MOF (**1**) in (a) single crystal form and (b) bulk powder form under N_2 atmosphere over the temperature range 30-500 °C at heating rate of 2 °C/min.

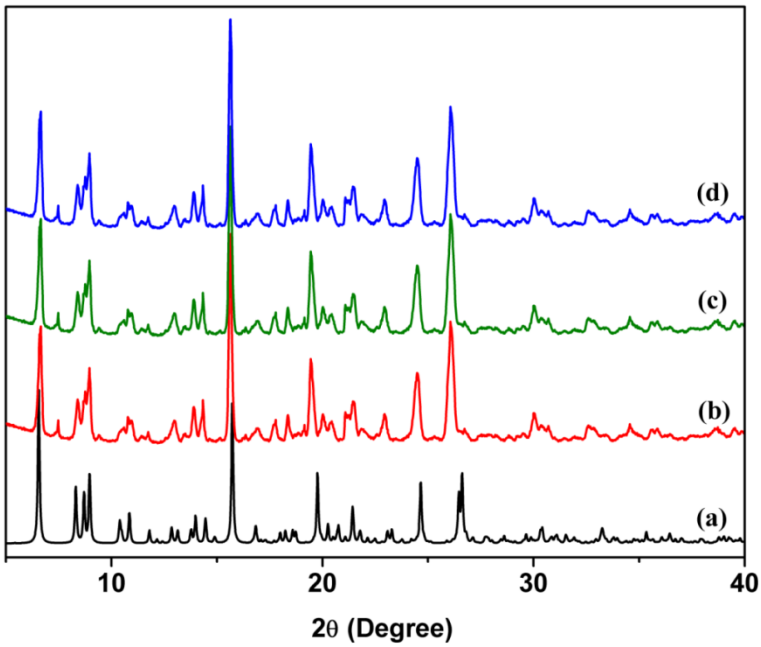

Fig. S6 PXRD patterns of Cd-MOF (**1**) in different states. (a) Simulated from X-ray single crystal data; (b) bulk as-synthesized compound; (c) activated compound at 70˚C; (d) activated compound at 170˚C. All major peaks of simulated PXRD patterns matched well with PXRD patterns of bulk as-synthesized compound and as well as activated compounds after dehydration (70 ˚C) and in film preparation temperature (170 ˚C). These indicate the crystalline phase purity of the bulk and activated samples.

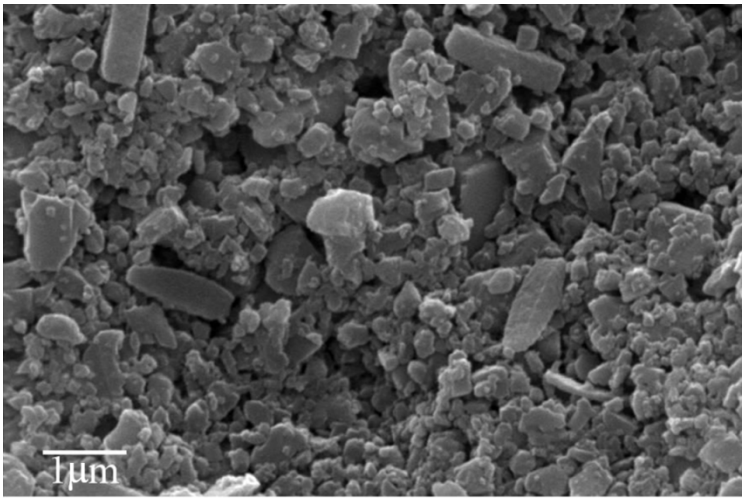

Fig. S7 SEM image of the powder sample of Cd-MOF (**1**).

Experimental and simulated optical spectra of Cd-MOF (**1**)

The solid state UV-vis absorption intensity of Cd-MOF (**1**) is recorded in the range of wavelength, 450nm to 900nm and plotted. Inset of Fig. S8 represents the spectrum. The completely diminished absorption curve after 600 nm indicates the absence of impurity energy level transition. The absorption coefficient (α) is estimated from the equation:

$$\alpha = -\frac{1}{t} ln\left(\frac{I_t}{I_0}\right)$$

Where t, I_t, and I_0 represent the thickness of the thin film of material, intensity of transmitted light, and intensity of incident light. The direct optical band gap of the material is estimated by Tauc's equation:[7]

$$(\alpha h\gamma)^{1/n} = C\left(h\gamma - E_g\right)$$

Where h is Planck's constant, C is proportionality constant, γ is the frequency of light, E_g is the band gap energy, and n = 1/2 for direct transition mode material. Fig. S8, depicts Tauc's plot, where $(\alpha h\gamma)^2$ is plotted against the photon energy (hγ) and the band gap energy is estimated as 2eV from the extrapolated line as shown.

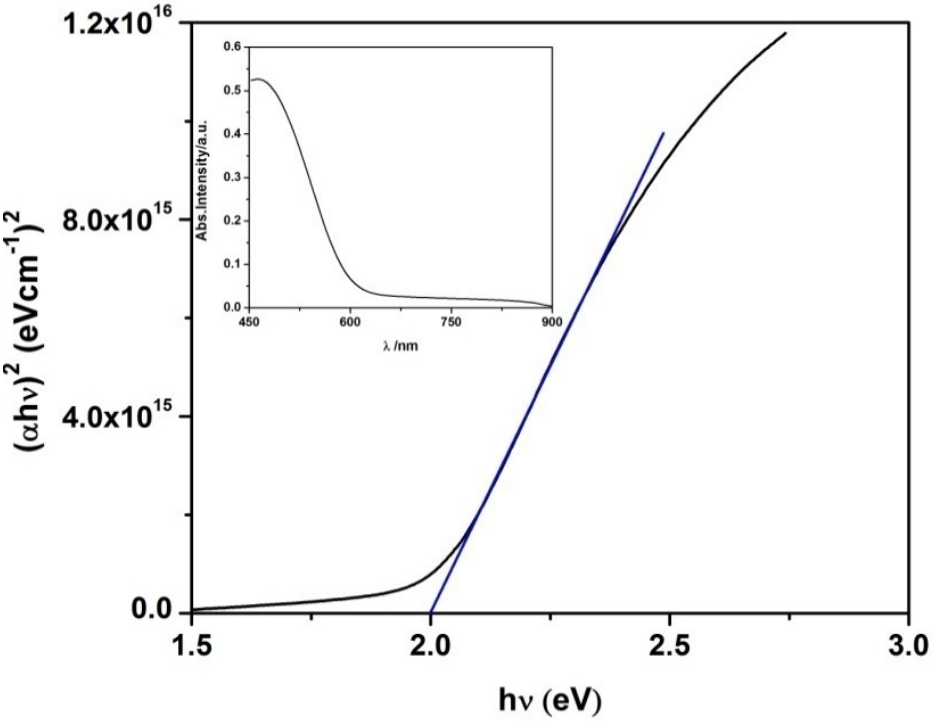

Fig. S8 UV-VIS absorption and Tauc's plot of Cd-MOF (**1**).

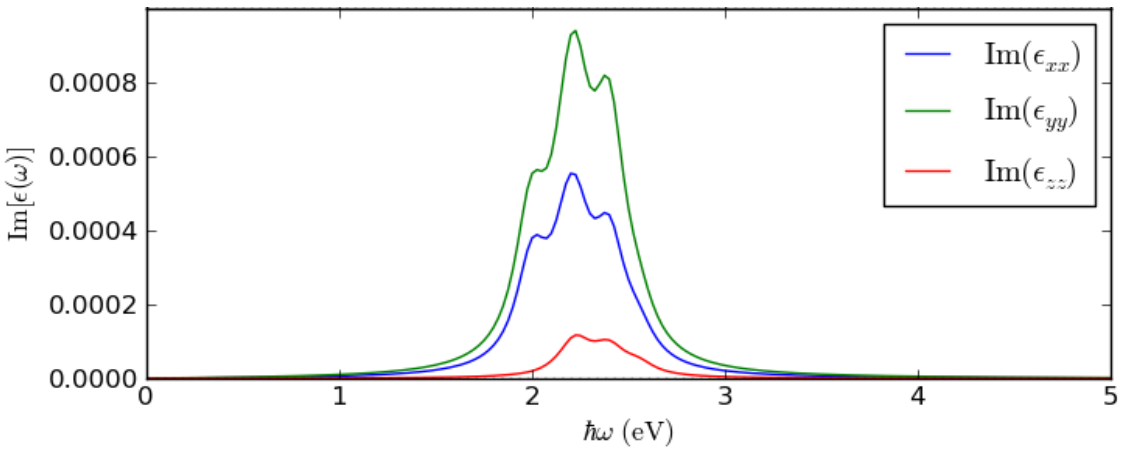

Fig. S9 Theoretical optical absorption spectra of Cd-MOF (**1**).

The imaginary tensor components of the frequency depended dielectric constant are plotted separately in the energy range 0 to 5eV. The figure illustrates that the yy component is the most intense one and the maximum of the peak appears at 2.2 eV. It is worth commenting that, the predicted fundamental band gap at the symmetric 'X' point of the Brillouin zone is 2.07eV. In principle, during an excitation process, if the electron-hole Coulomb interaction (excitonic effect) is strong, significant departure of the excitation peak having lower excitation energy in comparison to the fundamental gap should occur. The similarity in the fundamental gap with that of the linear response theory based excitation gap clearly indicates that the excitonic effect/quantum many-body effect is not operating here. Therefore, one can reasonably accept the optical gap of the Cd-MOF (**1**) as its fundamental gap. This theoretical finding actually justifies the evaluation of the band gap from the tail of the experimental absorption spectra.

Device Characterization

Electrical properties of the device ITO/ Cd-MOF (**1**)/Al have been investigated by current-voltage (I-V) measurement at room temperature (300K) in vacuum under dark conditions. The schematic sandwich structure of the device is shown in Scheme S2. The I-V characteristics of the device show rectifying behavior. To get further insight of the device, the I-V curve is analyzed for evaluating different device parameters and this has been done using the emission diffusion theory in combination with the equation of dependency of current on voltage for metal-semiconductor. The relevant equations are as follows:

$$I = I_0 \, exp\left(\frac{qV}{nKT}\right)\left[1 - exp\left(\frac{-qV}{KT}\right)\right] \quad (1)$$

$$I_0 = AA^* T^2 \, exp\left(\frac{-q\emptyset_b}{KT}\right) \quad (2)$$

$$n = \left(\frac{q}{KT}\right)\left[\frac{dV}{dln(I)}\right] \quad (3)$$

where n is the ideality factor, k is the Boltzmann constant, q is the electronic charge, A is the contact area, A^* is the Richardson constant, T is the temperature, I_0 is the saturation current in reverse bias and Φ_b is the potential barrier height. Employing the value of A^* as 0.248 for semiconductor material, the series resistance, ideality factor and barrier potential are determined by using Cheungs' equations:[8]

$$\frac{dV}{dln(I)} = \left(\frac{nKT}{q}\right) + IR_s \quad (4)$$

$$H(I) = V - \left(\frac{nKT}{q}\right) ln\left(\frac{I_0}{T^2 AA^*}\right) \quad (5)$$

and

$$H(I) = IR_s + n\emptyset_b \quad (6)$$

The series resistance and ideality factor are calculated from the slope and intercept of dV/dln(I) vs I plot (Fig. S10) and barrier height is evaluated from the intercept of H(I) vs I curve (Fig. S11).

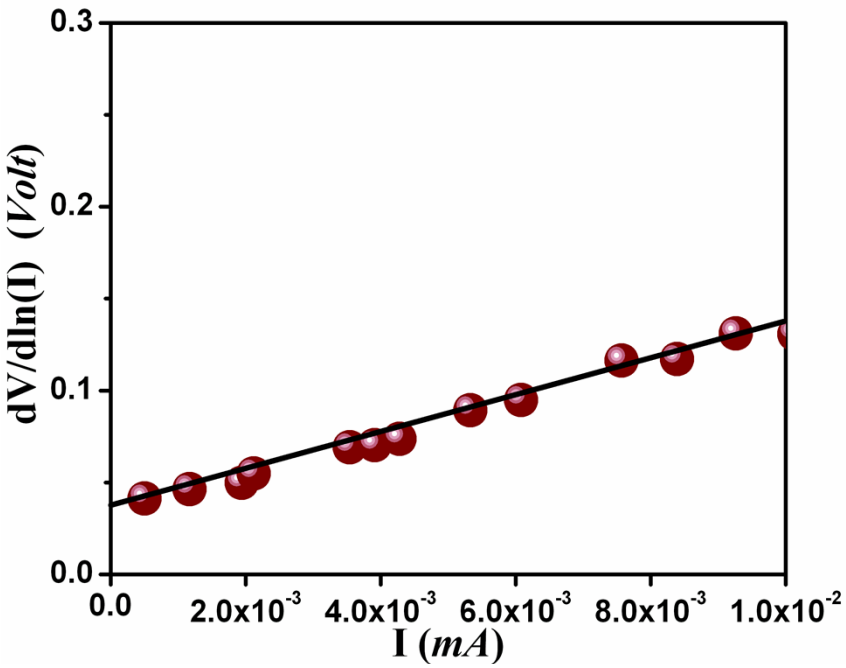

Fig. S10 dV/dln(I) vs I plot of ITO/Cd-MOF(**1**)/Al Schottky diode.

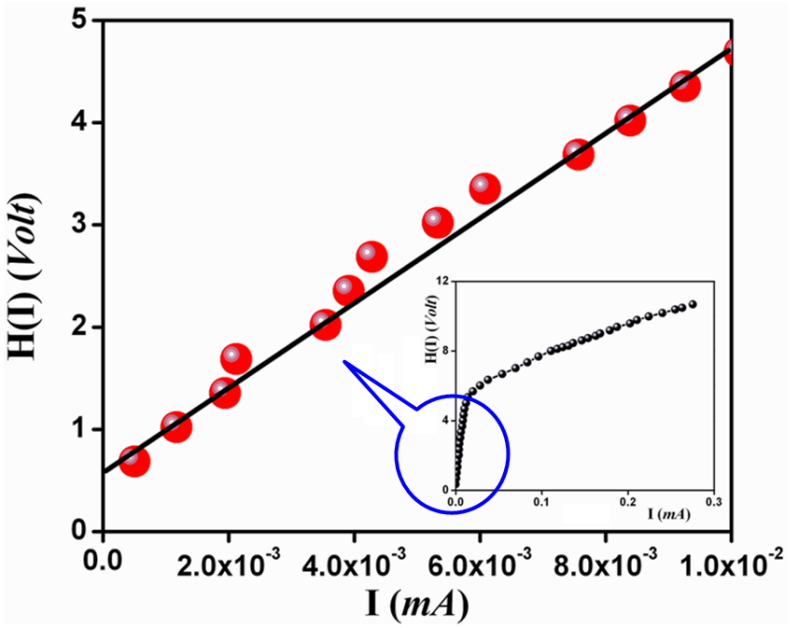

Fig. S11 H(I) vs I plot of ITO/Cd-MOF(**1**)/Al Schottky diode.

References:

1. O. Theilmann, W. Saak, D. Haase and R. Beckhaus, *Organometallics*, 2009, **28**, 2799.

2. G. M. Sheldrick, *Acta Cryst.*, 2008, **A64**, 112.

3. A. L. Spek, *Acta Cryst.*, 2009, **D65**, 148.

4. F. Tran and P. Blaha, *Phys. Rev. Lett.*, 2009, **102**, 226401.

5. http://www.quantumwise.com.

6. W. A. Harrison, *Solid State Theory*; McGraw-Hill Inc., 1970.

7. D. L. Wood and J. Tauc, *Phys. Rev. B.*, 1972, **5**, 3144.

8. S. K. Cheung and N. W. Cheung, *Appl. Phys. Lett.*, 1986, **49**, 85.